Design of Small Monitoring ROV for Aquaculture

Miao Yang
The Department of Electronic Engineering of Huaihai Institute of Technology,
Lianyungang, China.
Institute of Marine equipment, Jiangsu University of Science and Technology,
Zhenjiang, China.
lemonmiao@gmail.com

Zhibin Sheng
The Department of Mechanical and Ocean Engineering of Huaihai Institute of Technology,
Lianyungang, China.
abinwa@163.com

Yanhe Che
The Department of Electronic Engineering of Huaihai Institute of Technology,
Lianyungang, China.
718022614@qq.com

Jintong Hu
The Department of Mechanical and Ocean Engineering of Huaihai Institute of Technology,
Lianyungang, China.
hjt2218@outlook.com

Ke Hu
The Department of Mechanical and Ocean Engineering of Huaihai Institute of Technology.
Lianyungang, China.
kexisibest@outlook.com

Yixiang Du
The Department of Electronic Engineering of Huaihai Institute of Technology.
Lianyungang, China.
duyixiang94@outlook.com

***Abstract*—This work addresses a realization of a compact ROV (Remotely Operated Vehicle) for monitoring in a dark and turbid aquaculture environment. A six degree-of-freedom ROV with four thrusters is implemented, in which a novel structure is proposed to solve the heeling problem better. In addition, a lighting system with wide and uniform light field and a biaxial imaging platform are designed based on the principle of convex lens scattering analysis. The simulation and tank experiment results illustrate the effectiveness of the designed ROV on steadily and flexibly. It achieves moving forward at a velocity of 0.17m/s at 50HZ artificial flow, and cruising at a fixed depth with up to 5 hours battery life. The designed ROV exhibits better comprehensive performance than other small ROVs for the turbid aquaculture environments.**

Keywords—ROV; aquaculture; novel structure; lighting system;

I. INTRODUCTION

ROVs, as intelligent tools, have been widely used in marine explorations and aquaculture [1-3]. Some ROVs are listed in Table I. Although the existed ROVs have shown good performance in speed and control system, some limitations make it can not be applied to the aquaculture which needs the ROV have characteristics such as small size, corrosion resistance and stable motion to resist wave. Furthermore, some creatures in aquaculture, e.g. catfishes, lobsters, crabs and squids live in dark environment, which needs the imaging system equipped on the ROVs to be adaptive to a low light environment.

PID (Proportion Integral Derivative) control system have been widely applied in the controls of heading and depth of ROV motions [4-5]. However, PID control relies on the model of underwater vehicle dynamics. Xing *et al.* [6] utilized the SMC (Sliding Mode Control) to control pitch angle of the ROV, while the chattering problem of SMC has a serious impact on the control effect. García-Valdovinos *et al.* [7] proposed a new model-free second order SMC to improve the chattering problem. In addition, Mahapatra *et al.* [8] analyzed the H_∞ control for tracking the desired yaw angle accurately. Nonetheless, H_∞ control also has a disadvantage of low steady-state accuracy. Since it is difficult to achieve the desired control effect by a single control method, more combined approaches have been applied [9-10]. Sarhadi *et al.* [10] proposed a model reference adaptive PID control to the six degree-of-freedom nonlinear motion of an underwater vehicle. Khodayari *et al.* [11] applied an adaptive fuzzy PID control to prescribe the heading and depth of the ROV. Cui *et al.* [12] adopted an adaptive sliding-mode attitude control for yaw and pitch of underwater vehicle. Hosseini *et al.* [13] integrated a feedback linearization and model referenced adaptive control (MRAC) to administrate the horizontal plane cruising of the vehicle. Li *et al.* [14] combined an ellipsoidal exterior with a PD controller to resist the strong current. Although many improved methods have been used to control the motion of ROVs, these methods are complex, and part of them are still in the simulation stage.

This work was supported in part by the National Natural Science Foundation under Grant 61601194, the "Six talent peaks" project in Jiangsu Province (No. DZXX-030), and in part by Lianyungang "521" funded project, "Haiyan" funded project, and Jiangsu university of science and technology (high-tech ship) collaborative innovation center science and technology project, and in part by 2018 Graduate student scientific research and practice innovation projects in Jiangsu province(KYCX18_2596), 2019 Graduate student scientific research and practice innovation projects in Jiangsu province.

TABLE I THE PARAMETERS OF SOME COMMERCIAL ROVs

Type	*Size/mm³*	*weight/ kg*	*depth /m*	*The main application*
LBV 300-5 [15]	520×445×260	<13	300	Marine safety, Port security
AC-ROV [16]	203×152×146	<3	75	Check dam, Aquaculture
Video Ray Explorer [17]	310×230×210	<5	75	Underwater observation
Video Ray Voyager [17]	370×280×220	<6	76	Underwater observation
Steelhead [18]	384×502×373	<21	300	Underwater salvage
Globefish IV [19]	740×420×390	<25	300	Underwater observation
Robo-ROV [20]	510×490×400	<28	300	Check dam, Aquaculture
Robotfish [21]	450×290×220	<7.5	150	Underwater observation
SeaScan MK2 [22]	1580×500×430	<50	300	Pipeline inspection

In this paper, a monitoring ROV based on the requirements of aquaculture including small size, stability, long battery life and special lighting equipment is designed. The specific contributions of this paper are: (i) a six degree-of-freedom ROV with only four thrusters is implemented; (ii) a novel structure combined with cascade PID control is proposed to solve the heeling problem in ROV horizontal moving; (iii) a lighting system with wide and uniform light field and a biaxial imaging platform are designed upon on the principle of convex lens scattering analysis to get a better visual effect of underwater objects.

The rest of the article is organized as follows: Section II describes the mechanical design of the ROV, and provides a novel method to solve the heeling problem. In Section III, ROV dynamic model and equation of motion are analyzed. Furthermore, the system transfer function and the simulation results of ROV yaw angle are presented in Section IV. Section V illustrates the design of observation system including a lighting system with wide and uniform light field. The experiment and discussion are presented in Section VI. Section VII is conclusion.

II. STRUCTURE OF ROV

The structure of the designed ROV is shown in Fig. 1.

(a) Front view (b) Side view

Fig. 1 The monitoring ROV.

It consists of ground station and underwater actuator. The control station transmits signal to the power carrier module through WIFI or Ethernet, then the power carrier module, which is inside in the vehicle, transcodes the signal to the ROV, realizing the control of lighting equipment, sensors, camera and thrusters. The transmission of the system signal is shown in Fig. 2.

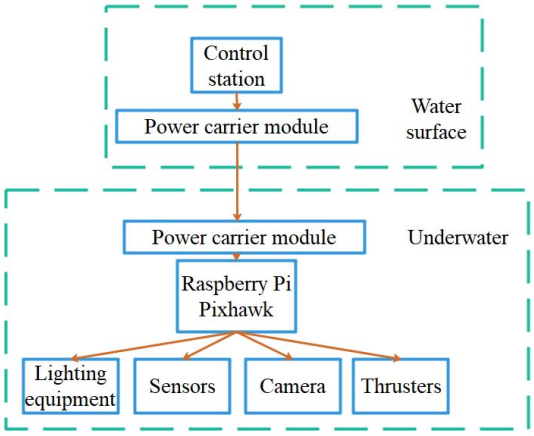

Fig. 2 The transmission of the system signal.

The characteristics of the designed ROV are as follows:

(1) Size: length 440mm×width 260mm×height 248mm.

(2) Weight: 3kg (approximately).

(3) Maximum depth of diving: 50m.

(4) Four thrusters: two lateral and two at the rear.

(5) One camera on the front.

A. Pressure Hull

A cylindrical pressure hull with a hemispherical head were adopted and sealed with a hollow flange in order to maximize the space of the pressure hull. The thickness of pressure hull is 5mm and the material is acrylic. Suppose the maximum of working depth is h_w and h_w=50m, the maximum of working pressure P_w is:

$$P_w = \gamma h_w . \tag{1}$$

where, γ is the density of water, γ=9.8kg/m^3. And $P_w=\gamma h_w=0.0098h_w$.

The computed pressure P_c is:

$$P_c = kP_w \tag{2}$$

where, k is defined as the safety coefficient and is equal to 1.3~1.6 empirically. Here, we take k=1.4. and P_c=0.686MPa.

The length, thickness and external diameter of the designed pressure hull is L=300mm, t=5mm, D=90mm, respectively.

$$L = 300mm < 4D\sqrt{\frac{D}{2t}} = 1080mm . \tag{3}$$

Based on Eq. (3), the designed ROV is belong to a short cylinder. The critical pressure P_{cr} can be computed by B. M. Pamm [23]:

$$P_{cr} = \frac{2.59E_t}{LD\sqrt{D/t}} . \tag{4}$$

where, E_t is the tangent modulus of the material, E_t=3GPa. By Eq. (4), P_{cr}=6.7MPa>>P_c=0.686MPa. Therefore, the suffered pressure of the designed ROV in 50m water is far less than the critical pressure that the pressure hull can sustain.

B. Thrusters

The performance of the thruster plays a significant role in the ROV system. There are many different types of the thrusters, for example, jet pumps [24]; modified bilge pumps; and brushless direct current (BLDC) motor based thruster [25]. In this work, we use the brushless DC motor based thrusters. The specs of the thrusters are given in Table II.

TABLE II THE SPECS OF THE THRUSTERS.

Maximum Current	30A
Voltage	12V-26V
PWM	1000-2000Hz
Frequency	50Hz

The thrust can be calculated by [26]:

$$T = \rho n^2 K_T D_T^4 . \tag{5}$$

where ρ *is* the density of water, K_T is the coefficient of thrust, D_T is the thruster disk diameter.

Generally, n thrusters are needed for a n-degree-of-freedom vehicle [23], such as LBV 300-5, Globefish IV, Robo-ROV. On the contrary, in this works, the designed ROV is equipped by 4 thrusters and realizes a movement in six degree of freedom, which reduces the size and the consumption of power. The distribution of thrusters is shown in Fig. 3. Figs. 3(a) and (b) are the diagrams of the distributions of horizontal and vertical thrusters, respectability. As shown in Fig. 3(c), T_1, T_2, T_3, T_4 are the thrust that generated by the thrusters.

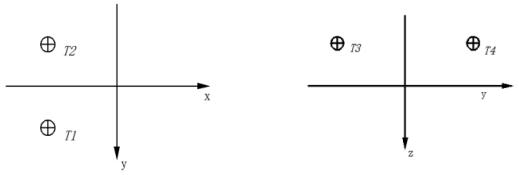

(a) Horizontal thrusters (b) Vertical thrusters

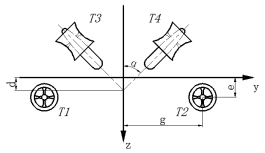

(c) The thrust of thrusters

Fig. 3 The distribution of thrusters.

Let M represents the moment, T represents thrust, then M and T can be calculated as [23]:

$$\begin{pmatrix} T \\ M \end{pmatrix} = \begin{pmatrix} \sum_{i=1}^{4} T_i \\ \sum_{j=1}^{4} T_j \end{pmatrix} = \begin{pmatrix} T_1 + T_2 \\ -(T_3 + T_4)\sin\alpha \\ (T_3 + T_4)\cos\alpha \\ d(T_3 - T_4)\sin\alpha \\ e(T_1 + T_2) \\ g(T_2 - T_1) \end{pmatrix} . \tag{6}$$

C. Heeling Problem

The force analysis of the traditional small ROV when it moves to right is illustrated in Fig. 4. It can be seen that the f_1 and f_2 are the forces generated by the vertical thrusters. F_1 is compounded by f_1' and f_2', F_2 is the hydrodynamic drag force. When the ROV moving to the right, the f_1'' and f_2'' acting on the both sides of the ROV would cause the ROV heeling to the right. In addition, the wave makes the rolling problem more worse.

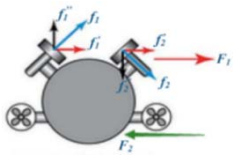

Fig. 4 Front view of the traditional small ROV.

The proposed structure is shown in Fig. 5. In this work, the vertical thrusters of the ROV are outward tilted 45° and a plastic sheet (yellow circle) is equipped under the ROV, as shown in Fig. 5(a). The force analysis of the designed ROV when it moving to right is shown in Fig. 5(b). It can be seen that the hydrodynamic drag force is reduced by the plastic sheet that makes the ROV works stably.

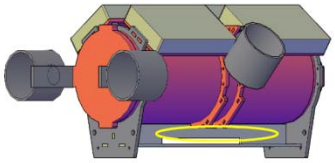

(a) Side view of the proposed ROV

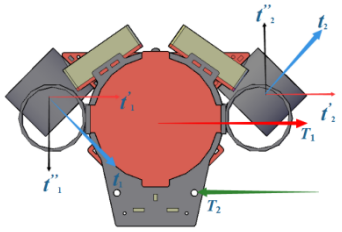

(b) Front view of our proposed ROV

Fig. 5 The diagram of the monitoring ROV.

III. ROV DYNAMICS

The definition of the reference coordinate frames of the ROV motion is shown in Fig. 6, where $X_oY_oZ_o$ is the earth-fixed frame and XYZ is the body-fixed frame [27]. The body-fixed frame is bonded to ROV where its origin is at the ROV center of gravity. The vector $V = [u\ v\ w\ p\ q\ r]^T$ is the velocity vector, the variables u, v and w are surge, sway and heave linear velocity, respectively, and p, q, r are angular rates in roll, pitch and yaw. The vector $\eta = [\eta_1\ \eta_2]^T = [x\ y\ z\ \varphi\ \theta\ \psi]^T$ is position vector, and x, y, z are the orientation of ROV in the earth-fixed frame, ϕ, θ, ψ represent the angle of ROV.

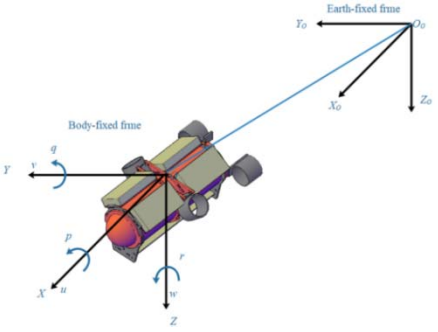

Fig. 6 Frame coordinates of the ROV.

Since the data that read by accelerometer and gyroscope are in the body-fixed frame, it is necessary to obtain the attitude information in the earth-fixed frame by rotation matrix. The rotation matrix as follows:

$$J(\eta) = \begin{pmatrix} J(\eta_1) & 0 \\ 0 & J(\eta_2) \end{pmatrix} \tag{7}$$

where $J(\eta_1)$ is the rotation matrix of the linear velocities vector and $J(\eta_2)$ is the rotation matrix of the angular velocities vector. $J(\eta_1)$ and $J(\eta_2)$ are given as:

$$J(\eta_1) = \begin{pmatrix} \lambda_1 & \lambda_2 & \lambda_3 \end{pmatrix}. \tag{8}$$

$$J(\eta_2) = \begin{pmatrix} 1 & \sin\varphi\tan\theta & \cos\varphi\tan\theta \\ 0 & \cos\varphi & -\sin\varphi \\ 0 & \sin\varphi/\cos\theta & \cos\varphi/\cos\theta \end{pmatrix}. \tag{9}$$

In Eq. (8), λ_1, λ_2 and λ_3 are column vectors, and expressed as follows:

$$\lambda_1 = \begin{pmatrix} \cos\varphi\sin\varphi \\ \sin\psi\cos\theta \\ -\sin\theta \end{pmatrix}. \tag{10}$$

$$\lambda_2 = \begin{pmatrix} -\sin\psi\cos\varphi + \cos\psi\sin\theta\sin\theta \\ \cos\psi\cos\theta + \sin\varphi\sin\theta\sin\psi \\ \sin\varphi\cos\theta \end{pmatrix}. \tag{11}$$

$$\lambda_3 = \begin{pmatrix} \sin\psi\sin\varphi + \cos\psi\cos\varphi\sin\theta \\ -\cos\psi\sin\varphi + \sin\theta\sin\psi\cos\varphi \\ \cos\theta\cos\varphi \end{pmatrix}. \tag{12}$$

The six degree-of-freedom of the ROV between the body-fixed frame and the earth-fixed frame are expressed as [26]:

$$\dot{\eta} = J(\eta)V\ . \tag{13}$$

By ignoring the coupling of vertical and horizontal planes, the equations of motion of the six degree of freedom are given as follows [24]:

$$X = m(\dot{u} - vr - x_g r^2 - y_g \dot{r}) \quad (14)$$

$$Y = m(\dot{v} + ur - y_g r^2 - x_g \dot{r}) \quad (15)$$

$$Z = m(\dot{w} - uq - z_g q^2 - x_g \dot{q}) \quad (16)$$

$$K = I_x \dot{p} + m[y_g(\dot{w} + vp) - z_g(\dot{v} - wp)] \quad (17)$$

$$M = I_y \dot{q} + m[z_g(\dot{u} + wq) - x_g(\dot{w} - uq)] \quad (18)$$

$$N = I_z \dot{r} + m[x_g(\dot{v} + ur) - y_g(\dot{u} - vr)] \quad (19)$$

where, x_g, y_g and z_g are the coordinates of the center of gravity of ROV, the variables $\dot{u}$, $\dot{v}$, $\dot{w}$, $\dot{p}$, $\dot{q}$, $\dot{r}$ are the derivative of linear and angular velocity, respectively. I_x, I_y, I_z are the moments of inertia on XYZ axes.

In this paper, we only studied the yaw of ROV. Because the center of gravity of ROV coincides with the origin of the body-fixed frame, the equations of motion can be simplified as:

$$X = m(\dot{u} - vr) \quad (20)$$

$$Y = m(\dot{v} + ur) \quad (21)$$

$$Z = m\dot{w} \quad (22)$$

$$N = I_z \dot{r} . \quad (23)$$

IV. CONTROLLER DESIGN

In this section, closed-loop transfer function of the ROV is deduced in detail. Then the cascade PID is adopted to control yaw of ROV. Finally, the performance of cascade PID is compared with conventional PID by simulation.

A. System Transfer Function

Supposing the thrusters which are on the horizontal plane have the same thrust, and the total thrust can be expressed as:

$$M = 2T = 2\rho n^2 K_T D_T^4 . \quad (24)$$

The drag moment of the ROV is given as follows:

$$M_D = 1/2\rho r^2 S N_r \quad (25)$$

where, r is the angular velocity, N_r is the drag coefficient and S is the equivalent area. The moment produced by inertial force when the ROV yaws is given as follows:

$$M_{\dot{r}} = m_{\dot{r}} \dot{r} . \quad (26)$$

where, $m_{\dot{r}}$ represents the added mass. According to Eqs. (23) - (26), the equation of motion when ROV yaws can be expressed as:

$$2\rho n^2 D^4 K_T - (-1/2\rho r^2 S N_r) = m_{\dot{r}} \dot{r} + I_z \dot{r} . \quad (27)$$

Considered that the model is a nonlinear system, and the angular velocity r is low, we deduce from Taylor expansion at $r=0$ for r^2, and Eq. (24) can be simplified as:

$$\frac{M}{m_{\dot{r}} + I_z} = \ddot{\varphi} . \quad (28)$$

In Eq. (28), $\ddot{\varphi}$ is second order derivative of the yaw angle, and the transfer function of yaw can be achieved by Laplace transform:

$$G_1(s) = \frac{\varphi(s)}{M(s)} = \frac{1}{s^2(m_{\dot{r}} + I_z)} . \quad (29)$$

The transfer function of the DC brushless motor can be expressed as:

$$G_2(s) = \frac{K}{Cs + 1} \quad (30)$$

where, C is time constant and K is transfer coefficient. The closed-loop transfer function of the system can be expressed as:

$$G(s) = \frac{G_1(s)G_2(s)}{1 + G_1(s)G_2(s)} . \quad (31)$$

B. Simulation and comparison

In this work, the cascade PID control is adopted, and the simulation platform is built by MATLAB/Simulink. The control flow diagram and the simulated response curves of the yaw angles are shown in Figs. 7 and 8. Fig. 8(a) is the result of the conventional PID control and Fig. 8(b) is the result of cascade PID. It can be seen that the setting time t_s in Fig. 8(b) is about 3s which is faster then the 6s in Fig. 8(a). Furthermore, the overshoot in Fig. 8(b) is much smaller than that in Fig. 8(a). All of these demonstrate that cascade PID has a faster response, and is superior to the conventional PID in performance.

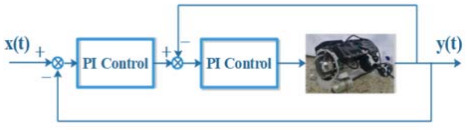

Fig. 7 The control diagram of the designed ROV.

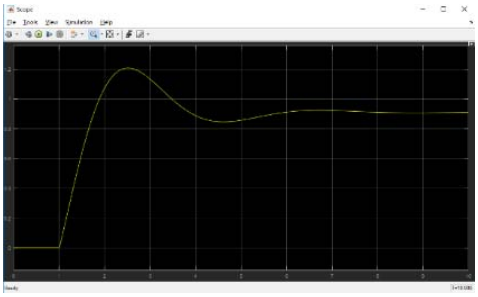

(a) Response of conventional PID

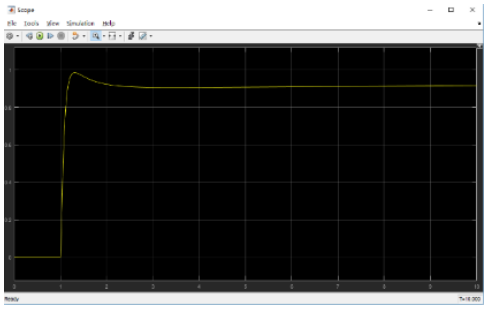

(b) Response of cascade PID

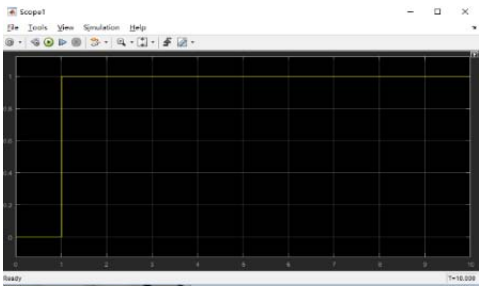

(c) Step signal

Fig. 8 Response curves of the yaw angle.

V. OBSERVATION SYSTEM

Because of the deposition of aquatic products' excreta and silt in the aquaculture, the water is commonly turbid. At the same time, there is low visibility under water especially at the seeding stage. In terms of these problems, a lighting system with wide and uniform light field and a biaxial imaging platform are presented in this section.

A. Lighting System

The illumination of the traditional Lamp-cup type underwater light is usually uneven due to the influence of impurities and suspended solids in the water, which creates a bright spot in the center of the image and darker area around it, as shown in Fig. 9(a). It will also produce the uneven illumination for an enlarged and deepen reflex cup, as shown in Fig. 9(b).

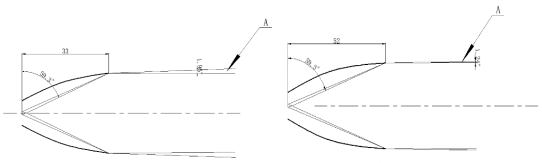

(a) (b)

Fig. 9 Lamp-cup type underwater light.

To solve this problem, convex lens is used as lamp shade in this work, which makes the light source spread evenly and avoids reflection of the collimating light under water, as shown in Fig. 10(a). It also guarantees a certain degree of pressure resistance because the convex lens was made of acrylic. In order to ensure the corrosion resistance, the shell of lamp was made of anti-rust aluminum alloy. The underwater light is shown in Fig. 10(b).

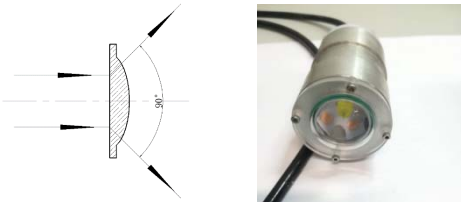

(a) Convex lens scattering (b) Appearance of underwater light

Fig. 10 Underwater light.

B. Camera System

For realizing the steady shooting, the designed ROV is equipped with a biaxial imaging platform that has two degree-of-freedom in pitch and roll, as shown in Fig.11. The angle of roll is between ±90° and the pitch is between ±45°.

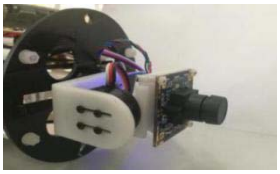

Fig.11 The bi-axial imaging platform.

VI. EXPERIMENT AND DISCUSSION

The experimental tank is 70m long and 1.5m wide. The water depth is 1.8m. In the experiment, the motions of yaw, pitch, roll, forward and backward, translation, diving were tested. The stability of the ROV was tested by artificial flow resistance system, as shown in Fig. 12(a), and the ROV moved smoothly forward at a speed of 0.17m/s at 50HZ artificial flow, as shown in Fig. 12(b).

The velocities of the ROV moves forward under different levels of artificial flow are shown in Table

III and IV. The parameters of the designed ROV and other commercial ROVs are compared in Table □. It can be seen from the Table III that the maximum velocity of the designed ROV when moving forwards is 1.42m/s, and it can achieve moving smoothly forward at a velocity of 0.17m/s at 50HZ artificial flow. From the Table IV, we can see that the maximum translation velocity of the designed ROV is 0.65m/s, and a velocity of 0.22m/s at 10Hz artificial flow can be attained when transverse moving is carried out. The data listed in Table V illustrates that the designed ROV has synthetic advantages in weight, size and velocity than other small ROVs. In addition, the designed lighting system realizes a uniform illuminating with 2000lm. And the camera system can shoot automatically with a ±90° rolling angle and ±45° pitching angle. The designed ROV can potentially be applied to reservoir, embankment, port engineering, and underwater rescue monitoring.

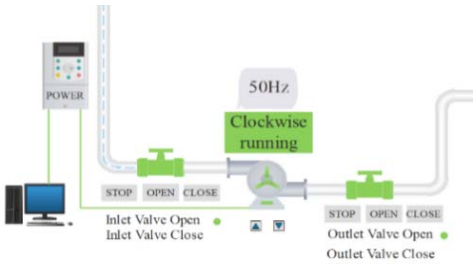

(a) The artificial flow resistance system

(b) ROV moves forward under artificial flow

Fig. 12 ROV testing in tank.

TABLE III THE FORWARD VELOCITY OF THE ROV AT DIFFERENT LEVELS OF ARTIFICIAL FLOW.

Velocity (m/s)	*The level of artificial flow (Hz)*
1.42	0
1.03	10
0.71	20
0.46	30
0.28	40
0.17	50

TABLE IV THE TRANSLATION VELOCITY OF THE ROV AT DIFFERENT LEVELS OF ARTIFICIAL FLOW.

Velocity (m/s)	*The level of artificial flow (Hz)*
0.65	0
0.22	10

TABLE V THE PARAMETERS OF THE DESIGNED ROV AND OTHER COMMERCIAL ROVs.

	Size (mm)	*Weight (kg)*	*Lighting (lm)*	*Speed (knot)*
The designed ROV	440×260×248	3	2000	3
Robo-ROV	510×490×400	28	700	3
vLBV300	625×390×390	18.1	2160	3
Sea ROVER	870×660×690	47	700	2.5
Mini ROVER	298×406×686	23.5	800	4

VII. CONCLUSION

In this article, a six degree of freedom monitoring ROV for dark and turbid aquaculture environment was designed and tested. The ROV is equipped with four thrusters, has a size of 440×260×248mm, weighs about 3kg. The maximum dive depth is 50m and the maximum velocity of the designed ROV when moving forwards is 1.42m/s. Besides, it can achieve moving smoothly forward at a velocity of 0.17m/s at 50Hz artificial flow. The maximum translation velocity of the designed ROV is 0.65m/s, and translation velocity at 10Hz artificial flow is 0.22m/s. The experiments validated the decent synthetic performance of the designed ROV. In the future, the ROV will be equipped with variety of sensors, for example, water temperature sensor, pressure sensor, gyro sensor, electronic compass, and be applied to inspect reservoir, dam, harbor, ships and the like.

REFERENCE

[1] H T Choi, J Choi, Y Lee, *et al*. "New concepts for smart ROV to increase efficiency and productivity," in IEEE Underwater Technology (UT), Feb. 2015, pp. 1-4.

[2] E Anderlini, G G Parker, and G Thomas, "Control of a ROV carrying an object," Ocean Engineering, vol. 165, pp. 307-318, 2018.

[3] J Teague, M J Allen, T B Scott, "The potential of low-cost ROV for use in deep-sea mineral, ore prospecting and monitoring," Ocean Engineering, vol. 147, pp. 333-339, 2018.

[4] J Rojas, G Baatar, F Cuellar, *et al*. "Modelling and Essential Control of an Oceanographic Monitoring Remotely Operated Underwater Vehicle," IFAC-PapersOnLine, vol. 51, no. 29, pp. 213-219, 2018.

[5] S M Nornes, M Ludvigsen, A J Sørensen. "Automatic relative motion control and photogrammetry mapping on steep underwater walls using ROV," in OCEANS 2016 MTS/IEEE Monterey, Sept. 2016, pp. 1-6.

[6] R Y Xing, S W Ma, J P Zhong. "Modeling and Simulation of Remote Operated Vehicle Based on Simulink," System Simulation Technology, vol. 14, no. 2, pp. 26-29, 2018.

[7] L G García-Valdovinos, T Salgado-Jiménez, M Bandala-Sánchez, *et al.* "Modelling, design and robust control of a remotely operated underwater vehicle," International Journal of Advanced Robotic Systems, vol. 11, no. 1, pp. 1-16, 2014.

[8] S Mahapatra, B Subudhi. "Design of a steering control law for an autonomous underwater vehicle using nonlinear H∞ state feedback technique," Nonlinear Dynamics, vol. 90, no. 2, pp. 837-854, 2017.

[9] S A Gayvoronskiy, T Ezangina, I Khozhaev. "Providing a Robust Aperiodic Transient Process in Motion Control System Unmanned Underwater Vehicle with Interval Parameters," IFAC-PapersOnLine, vol. 51, no. 29, pp. 220-225, 2018.

[10] P Sarhadi, A R Noei, A Khosravi. "Model reference adaptive PID control with anti-windup compensator for an autonomous underwater vehicle," Robotics and Autonomous Systems, vol. 83, pp. 87-93, 2016.

[11] M H Khodayari, S Balochian. "Modeling and control of autonomous underwater vehicle (AUV) in heading and depth attitude via self-adaptive fuzzy PID controller," Journal of Marine Science and Technology, vol. 20, no. 3, pp. 559-578, 2015.

[12] R Cui, X Zhang, D Cui. "Adaptive sliding-mode attitude control for autonomous underwater vehicles with input nonlinearities," Ocean Engineering, vol. 123, pp. 45-54, 2016.

[13] M Hosseini, S Seyedtabaii. "Improvement in ROV horizontal plane cruising using adaptive method," in 24th Iranian Conference on Electrical Engineering (ICEE), 2016, pp. 1892-1896.

[14] J H Li, M G Kim, H J Kang, *et al.* "Development of UUV Platform and its Control Method to Overcome Strong Currents: Simulation and Experimental Studies," IFAC-PapersOnLine, vol. 51, no. 29, pp. 268-273, 2018.

[15] Teledyne SeaBotix ROVs. Available Online: https://imenco.no/product/seabotix-lbv-300-5/ (accessed on 23 April 2019)

[16] AC-CESS. Available Online: http://ac-cess.com/ (accessed on 23 April 2019)

[17] Videoray. Available Online: http://www.videoray.com/ (accessed on 23 April 2019)

[18] SEAMOR Marine Ltd. Available Online: https://seamor.com/ (accessed on 23 April 2019)

[19] Sublue. Available Online: http://www.deepinfar.com/ (accessed on 23 April 2019)

[20] Robsea. Available Online: http://www.robosea.org/ (accessed on 23 April 2019)

[21] Robothish Underwater robot. Available Online: http://www.chinarov.com/ (accessed on 23 April 2019)

[22] ECA GROUP. Available Online: https://www.ecagroup.com/en/solutions/Seascan-MK2 (accessed on 23 April 2019)

[23] X S Jiang. Unmanned underwater vehicle. Science and technology press of Liaoning, 2000.

[24] K Alam, T Ray, S G Anavatti. "Design and construction of an autonomous underwater vehicle," Neurocomputing, vol. 142, pp. 16-29, 2014.

[25] R S Duelley, Autonomous underwater vehicle propulsion design. Virginia Tech, 2010.

[26] J Kim, W K Chung. "Accurate and practical thruster modeling for underwater vehicles," Ocean Engineering, vol. 33, no. 5-6, pp. 566-586, 2006.

[27] T I Fossen. "Marine control system-guidance, navigation and control of ships, rigs and underwater vehicles," Marine Cybemetics, 2002.

Miao Yang (M'12) was born in Wu Chang City, Heilongjiang Province, China, in 1978. She received the B.S. and M.S. degrees in Electronic Engineering from LanZhou University, Gansu Province, China in 2004 and the Ph.D. degree in Information Science and Engineering from Ocean University of China, Qingdao, in 2009. From 2010 to 2013, she was a post-doctoral fellow with Internet of Things Engineering Department, Jiangnan University, China. Since 2009, she has been a Professor with the Electronic Engineering Department, HuaiHai Institute of Technology. She is currently cooperated with Qingdao National Lab. of Marine science and technology in underwater image understanding. She is the author of more than 30 articles and holds two patents. Her research interests include underwater vision, image processing, computer vision and 3D reconstruction.

Zhibin Sheng, He was born in Tai Zhou City, JiangSu Province, China, in 1994. He is currently pursuing the master's degree from the Department of Mechanical and Ocean Engineering of Huaihai Institute of Technology, Lianyungang, Jiangsu. He received the B.E. degrees in Mechanical and Ocean Engineering from Huaihai Institute of Technology, JiangSu Province, China in 2016. His current research interest is in the field of Remotely Operated Vehicle.

Yanhe Che, undergraduate student, He was born in Kunming City, Yunnan province, China, in 1995. Participated in the 7th national Marine vehicle design and production competition in 2018 and won the second prize

Jintong Hu, Postgraduate student, He was born in Nan Tong City, JiangSu Province, China, in 1993. He received the B.E. degrees in Electronic Information Engineering from Huaihai Institute of Technology, JiangSu Province, China in 2016.

Yixiang Du is currently pursuing the master's degree from the School of Information and Control Engineering, China University of Mining and Technology, Xuzhou,Jiangsu. He studied electronics and information engineering at Liaocheng University from 2012 to 2016. His research interests include image processing, 5G, and the machine learning

Ke Hu, Postgraduate student, He was born in Chang Ge City, HeNan Province, China, in 1993. He received the B.E. degrees in Electronic Information Engineering from Huaihai Institute of Technology, JiangSu Province, China in 2017. His research interests include image processing, and the machine learning.